Received: 22 November 2019 | Accepted: 21 February 2020

DOI: 10.1002/vzj2.20019

Vadose Zone Journal

ORIGINAL RESEARCH ARTICLE

Temperature response and brine availability to heated boreholes in bedded salt

Eric J. Guiltinan[1] | Kristopher L. Kuhlman[2] | Jonny Rutqvist[3] | Mengsu Hu[3] | Hakim Boukhalfa[1] | Melissa Mills[2] | Shawn Otto[4] | Douglas J. Weaver[4] | Brian Dozier[4] | Philip H. Stauffer[1]

[1]Earth and Environmental Sciences Division, Los Alamos National Lab., Los Alamos, NM, USA

[2]Applied Systems Research Department, Sandia National Lab., Albuquerque, NM, USA

[3]Energy Geosciences Division, Lawrence Berkeley National Lab., Berkeley, CA, USA

[4]Los Alamos National Lab., Carlsbad Field Office, Carlsbad, NM, USA

Correspondence
Philip H. Stauffer, Earth and Environmental Sciences Division, Los Alamos National Lab., Los Alamos, NM, USA.
Email: stauffer@lanl.gov

Funding information
USDOE, Grant/Award Number: 89233218CNA000001

Abstract

There is a growing need for disposal of high-level nuclear waste. To reduce uncertainty associated with brine availability to repository excavations in salt formations, a collaboration between Sandia, Los Alamos, and Lawrence Berkeley National Laboratories is performing a series of borehole-scale coupled process tests. Here, we report on the first round of the Brine Availability Test in Salt (BATS) project, a "shakedown" experiment called Phase 1s. Experimental testing included placing a resistive heater, a 260-W radiative heater, and a 750-W radiative heater within previously drilled horizontal boreholes at the Waste Isolation Pilot Plant (WIPP) while monitoring temperature and water inflow. The experiments successfully achieved the targeted temperature of 120 °C when using the 750-W radiative heater. Simulations using FEHM (Finite Element Heat and Mass transfer code) and TOUGH-FLAC (Transport Of Unsaturated Groundwater and Heat–Fast Lagrangian Analysis of Continua) were able to accurately predict the coupled thermo–hydro–mechanical–chemical response of salt, matching the observed temperature and brine production. Due to the extremely low permeability of salt, these systems take many years to reach steady state when perturbed by mining activities. Long-term numerical simulations are used to develop the initial pressure and saturation conditions. The inclusion of a damaged rock zone with higher permeability around the borehole also affects the saturation and pressure distributions and plays an important role in dissipating the potential for thermal pressurization. Knowledge gained from this round of experimentation and simulation will be used to conduct the next BATS project experiment in new boreholes at WIPP.

Abbreviations: BATS, Brine Availability Test in Salt; DRZ, damaged rock zone; FEHM, Finite Element Heat and Mass transfer code; HLW, high-level waste; TB, temperature borehole; TBO, temperature borehole sensor at position 0; 3D, three-dimensional; TOUGH-FLAC, Transport Of Unsaturated Groundwater and Heat–Fast Lagrangian Analysis of Continua; TSB, temperature small borehole; TSBO, temperature small borehole sensor at position 0; 2D, two-dimensional; WIPP, Waste Isolation Pilot Plant.

1 | INTRODUCTION

Worldwide, there exists ~2.8 million m^3 of high-level heat-generating nuclear waste (HLW) in temporary storage (IAEA, 2018), including 364,000 m^3 of HLW in the United States alone, where the volume of HLW waste continues to increase without a clear path to disposal. In the United States, the

USDOE Office of Nuclear Energy is funding research into the generic feasibility of HLW disposal in geologic repositories within competent crystalline rock formations, low-permeability argillaceous formations, and salt formations (UFD Campaign, 2012). Geologic salt formations may be an ideal host media for a HLW repository due to salt's extremely low permeability in the far field, high thermal conductivity, and self-healing capability (Hansen & Leigh, 2011; MacKinnon, Sevougian, Leigh, & Hansen, 2012). These characteristics have led to the selection of salt for two low- and intermediate-level waste repositories, the Waste Isolation Pilot Plant (WIPP), in New Mexico, USA, and the Morsleben Mine in Germany. Research into these repositories has provided an extensive foundation of knowledge and confidence regarding the containment provided by their respective formations (Kuhlman & Sevougian, 2013). Salt formations can make an excellent barrier to long-term release of radionuclides to the biosphere, but our ability to predict aspects of the short-term and near-field behavior of salt (i.e., operational and early post-closure phases of a future repository) would be enhanced by investigations into coupled thermal, hydrological, mechanical, and chemical behavior (Kuhlman, Mills, & Matteo, 2017; Stauffer et al., 2015).

Bedded salt deposits are relatively dry (<5% water by volume), but water does exist in salt formations within intragranular porosity as fluid inclusions, intergranular porosity (between halite crystal interfaces, in small fractures [Larson, 2000], in the porosity of clays and other non-halite minerals), and bound within hydrated minerals. Each of these three types of water have different mobilities, and they respond differently to temperature and pore pressure changes. Brine inflow in unheated mine excavations has been observed in both repositories despite salt's extremely low permeability and porosity (Bredehoeft, 1988; Geckeis & Klenze, 2009; Larson, 2000). At WIPP (bedded salt), brine accumulations have been shown to be similar in composition to intergranular water (Larson, 2000). At WIPP, the permeability of intact rock salt is estimated at 10^{-21} to 10^{-22} m^2, and in the far field, away from the disturbed section of the mine, the flow is thought to approach zero under natural hydraulic gradients (Beauheim, Domski, & Roberts, 1999). With low undisturbed permeability and intergranular porosity of halite at 0.1% (Beauheim & Roberts, 2002), the physical processes that drive the formation brine toward open boreholes and excavations, especially near sources of heat, remain a source of uncertainty (Bourret et al., 2019; Mills et al., 2019).

The high thermal conductivity of salt allows the heat generated from radioactive decay in HLW to be efficiently conducted into the formation, leading to lower repository temperatures at earlier periods compared with other potential disposal media. However, the tightly coupled nature of thermal–hydrological–mechanical–chemical processes in salt means that understanding the effects of this heat on other processes requires an all-encompassing approach. For example, temperature rise drives thermal pressurization, salt creeps in response to deviatoric stresses, the creep rate increases with temperature and humidity (Hansen & Leigh, 2011), the solubility of halite and other evaporite minerals generally increases with temperature, and the thermal conductivity of the salt itself decreases significantly with temperature (Sweet & McCreight, 1983). These processes are further complicated by the heterogeneous nature of the geologic salt. As mining or drilling activities perturb the stress state, fractures create a damaged rock zone (DRZ) with higher and more connected intergranular porosity. The increased porosity of the DRZ starts off mostly air-filled, and the increased directional permeability (fractures oriented parallel to excavation face) of the DRZ allows movement of water towards excavations and HLW canisters.

Core Ideas

- Drift-scale simulations can develop the unsteady initial conditions in salt.
- A damaged rock zone around the borehole significantly affects water inflow.
- Lower saturations within the damaged rock zone limit thermal pressurization.
- A 750-W radiative heater can achieve the targeted borehole temperature of 120 °C.

Coupled thermal–hydrological–mechanical–chemical processes also result in the movement of intragranular fluid inclusions toward sources of heat and an increase in formation pressure near heat. The solubility of salt increases with temperature. When heat is applied to a fluid inclusion, it begins to dissolve on the hotter side, and this dissolved salt moves through diffusion to the colder side, where it precipitates. As this process continues, the fluid inclusion migrates towards the source of heat (Anthony & Cline, 1971; Pigford, 1982). Coupled thermal–hydrological processes may lead to thermal pressurization around heat sources, due to thermal expansion of the brine and the low permeability of salt. The formation of this high pressure zone occurs just outside the DRZ surrounding the heat source and excavation (where permeability is lower and brine saturation is higher) because the thermal diffusivity is higher than the hydraulic diffusivity, allowing the heat to propagate more effectively than the resulting pressure pulse (McTigue, 1986).

Accurate numerical simulation of the thermal impacts of HLW on salt is important for understanding the long-term behavior of a potential underground repository. Unfortunately, simulating numerous coupled process in a multiphase deformable system with large pressure and temperature gradients, and variable porosity, is computationally challenging. To understand the system, simplifying assumptions are typically made, but because of coupled effects, the choice of which processes to represent and how is critical. As much as possible, numerical simulations designed to elucidate the effect of coupled processes on the evolution of the repository should represent the full physics (Kuhlman, 2019). In addition, the necessary scale of the experiments, large gradients, and boundary effects require a highly resolved three-dimensional (3D) mesh, which is computationally expensive. Simulating these coupled processes and calibrating them to field observations is an important part of reducing uncertainty in a future repository.

Observing the coupled responses of salt to heat and two-phase flow around HLW packages requires careful experimentation and monitoring (Stauffer et al., 2015). To demonstrate confidence in pre-closure drift-scale simulations of a future HLW salt repository, it is necessary to understand these processes and their effect on the availability of brine. Uncertainties associated with brine source, abundance, composition, and flow mechanisms in salt must be reduced. With this goal in mind, a USDOE Office of Nuclear Energy-funded collaboration between Sandia, Los Alamos, and Lawrence Berkeley National Laboratories is conducting heated borehole experiments in the WIPP underground (a USDOE Office of Environmental Management facility). Although WIPP is not being considered for HLW disposal, it does provide an excellent environment for conducting research on HLW disposal in salt.

Stauffer et al. (2015) proposed a series of staged thermal testing at WIPP. The Brine Availability Test in Salt (BATS) experiments are the first U.S. heater tests in salt in almost 30 yr and the first time a heated borehole experiment will be conducted in bedded salt without intersecting a significant clay layer. The results from the first stage of planned testing, a "shakedown" test known as Phase 1s, are presented here and were first described in Kuhlman et al. (2017). The results of these experiments have been used to develop a larger scale test, which is known as the Phase 1 test, and was described in detail by Mills et al. (2019). The Phase 1 test began January 2020 and will run for several months. First, we discuss previous work relevant to the BATS experiment, next we describe the Phase 1s experiment in detail, and finally we present the results and the numerical models developed to simulate these coupled processes. The goal of this modeling work is to develop and validate simulations of the temperature response and brine availability heat sources to reduce the uncertainty associated with storing heat generating nuclear waste in salt formations. Lessons learned and insights gained in this initial testing are proving vital to the design and implementation of the larger scale borehole heater experiment.

2 | HEATED BOREHOLE EXPERIMENTS

2.1 | Previous heated brine migration experiments in salt

Brine availability studies have been conducted at several different underground research laboratories around the world since the late 1950s (Kuhlman & Malama, 2013; Kuhlman & Sevougian, 2013). Here, we briefly introduce some historical tests, indicating where aspects of the current generation of tests were previously used (Kuhlman et al., 2017).

The earliest (1965–1967) major borehole heater test in salt that monitored brine inflow was conducted in three arrays of seven vertical boreholes into bedded salt deposits in the floor of the Carey Salt Mine near Lyons, KS (Bradshaw & McClain, 1971). These tests included electrical and radioactive sources (~10.5 kW total power in each array) and were conducted as part of Project Salt Vault. This test sequence pioneered the concept of measuring humidity of circulated dry N_2 gas to quantify the brine inflow to the borehole after trying other less-successful approaches. They observed significant increases in brine inflow rate during step changes (i.e., both increases and decreases) in applied power and observed higher brine production associated with non-salt layers intersecting the boreholes. Their Room 5 had extensive shale and anhydrite interbeds and produced 35 L of brine—up to three times more brine than other geometrically similar heater arrays in purer salt.

Heated brine migration field tests have been conducted in domal salt underground research laboratories in the United States (Avery Island, LA) and in Germany (Asse II Mine). Domal salt has typically about one-tenth as much brine as bedded salt (less clay content and fewer fluid inclusions). Brine migration experiments were conducted during 1979–1980 in three arrays of seven vertical boreholes at Avery Island (Krause, 1983). These experiments were the first to place dissolved (Mg^{2+} ion) and stable-water isotope (deuterated water) tracers. They had parallel heated and unheated tests, they overcored the central test borehole after the end of testing, and they found that much less brine was produced overall than in the bedded salt heater test in Kansas (<40 g brine per borehole array). Approximately half of the total brine produced in the synthetic brine array of the ~200-d tests occurred during the 6-d cool-down period after the heater was shut down. Gas permeability measurements were made both during the cool-down period and in vertical boreholes at different radial distances from a nearby long-term heater test (Blankenship & Stickney, 1983). The results of permeability testing showed that the hotter salt (53 vs. ambient 27 °C) had two orders of magnitude lower permeability (i.e., the DRZ associated with the drift had partially healed), and that permeability increased significantly (more than four orders of magnitude) during cool-down due to tensile fracturing (Kuhlman & Malama, 2013).

At the Asse II Mine in Germany, a large-scale heated brine migration study was performed in 1983–1985, which involved collaboration between U.S. and German parties (Coyle, Eckert, & Kalia, 1987; Rothfuchs et al., 1988). This test involved four arrays of boreholes (central heated borehole with surrounding guard heaters), with either radioactive or electrical heaters, being either sealed or circulating dry N_2 gas. Gas composition samples were collected downstream of a cold trap. Acoustic emissions and room closure measurements were made during the brine migration study. The central heated boreholes reached an approximate steady-state temperature of 200 °C after 200 d of heating. Much less brine was observed in the test than was expected. Less than 2 L of brine was collected in any array, the majority of the brine (∼90%) was collected during the month-long gradual cool-down phase of the test, and a large number of acoustic emissions were detected near the end of the cool down. Post-test sampling showed the salt was dry within 12 cm of the central heater.

From 1985 to 1990 at WIPP, four large-diameter heated vertical boreholes in two drift-scale disposal demonstrations were instrumented to measure brine inflow at two different power levels (McTigue & Nowak, 1987; Nowak & McTigue, 1987). These vertical boreholes intersected a horizontal clay layer that produced significant brine, and at steady state, the hotter boreholes (120 °C in boreholes with 1,500-W heaters) had a brine inflow rate (∼50–60 g d^{-1} per borehole) about six times that observed in cooler boreholes (9–10 g d^{-1} per borehole in 50 °C boreholes with 470-W heaters). The hotter boreholes produced much more brine than expected and overwhelmed the dry N_2 brine collection system, with significant condensation occurring in the gas plumbing outside the boreholes. Unfortunately, the tests were shutdown abruptly without collecting cool-down brine production data. The heater that produced the most brine failed early and was removed via overcoring. The initial gap between the heater and borehole wall was found to have filled with significant deposits of precipitated salt, consistent with the large amount of brine (∼35 L) collected (Krumhansl, Stein, Jarrell, & Kimball, 1991), showing that the boiling of brine near sources of heat can concentrate significant solid salt.

Extensive brine inflow observations were made in both small- and large-diameter unheated boreholes at WIPP (Deal et al., 1995; Finley, Hanson, & Parsons, 1992), which although unheated are mentioned here because of their relevance to the current phase of testing. Although there was a significant variability in observed brine flow rates across the facility horizon, nearly all boreholes flowed brine consistently after drilling, and brine production was often related to the clay content of the salt and whether or not the borehole crossed a non-salt anhydrite or clay unit. These brine inflow data have already been the subject of previous numerical modeling exercises (Beauheim et al., 1997; Freeze, Christian-Frear, & Webb, 1997).

2.2 | Brine availability test in salt

The BATS experiment marks the first heated borehole salt experiments conducted underground at WIPP since Room A and B heater tests ended in the early 1990s (Munson et al., 1990). With much of the tacit knowledge from the previous experiments having been lost to retirements, the early round of BATS experimentation involved several logistical and technical challenges. These challenges were foreseen at the outset, and thus the scope of the early experiments was limited to allow the team to gain experience working underground at WIPP before conducting more challenging experiments (Johnson, Stauffer, Zyvoloski, and Bourret, 2018; Kuhlman et al., 2017; Mills et al., 2019; SNL, LANL, & LBNL, 2020; Stauffer et al., 2015). The borehole testing discussed here began in June 2018 and was completed by May 2019.

Existing boreholes in the WIPP underground (drilled for core collection) were used to test different experimental components. The general test design included a heater isolated behind an inflatable packer, temperature sensors, and dry N_2 circulating behind the packer (Figure 1). The dry N_2 was circulated at 200 ml min^{-1} from a tank at the drift face, through the packer via an isolated gas inlet, exiting behind the heater. Next, the N_2 mixed with borehole air and exited through the packer via an isolated gas outlet. On the downstream side, the N_2 passed through containers of Drierite desiccant, which was weighed periodically to quantify water removal from the heated borehole. The water flow rate measurement from the desiccant was confirmed using inline measurements of relative humidity (capacitive sensor) and flow-rate before the desiccant. Temperature sensors (thermocouples and resistive temperature sensors) were deployed in the heated borehole and in two adjacent boreholes (temperature borehole [TB]; and temperature small borehole [TSB]). Sensors in adjacent boreholes were grouted in place using a cement slurry composed of 49.5% Portland cement, 12.5% granular salt, 5% attapulgite, and 33% water.

Testing initially relied upon a resistive heater embedded in a stainless-steel block set to a prescribed temperature, measured on the outside of the block. With a goal of producing a borehole wall temperature of 120 °C, the heater block was installed on 5 June 2018 and was set to 120 °C. However, the air gap around the heater block insulated the formation from the heater, creating a poor thermal coupling between the salt and heater. This resulted in observed temperatures within the

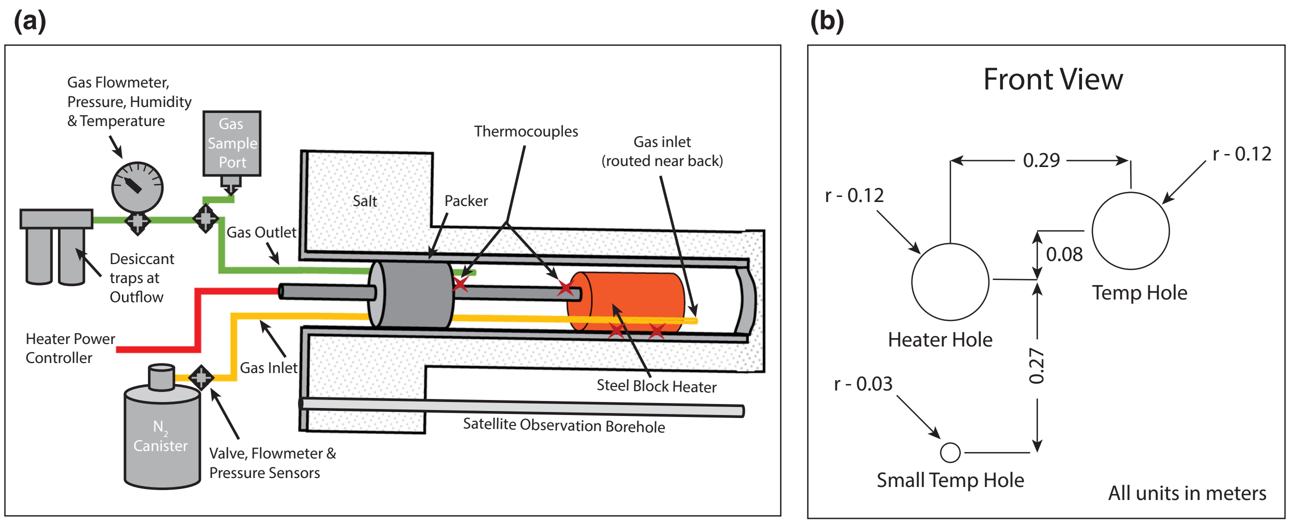

FIGURE 1 (a) Detailed side view of heated borehole instrumentation and (b) front view layout of heated borehole and two temperature monitoring boreholes temperature hole (TB) and small temperature hole (TSB)

FIGURE 2 Left: 750-W infrared heater being tested at Waste Isolation Pilot Plant (WIPP) prior to installation (heater element is 60 cm long). Right: Installation of the 750-W infrared heater in borehole

adjacent observation boreholes of only 35 °C, a 3.5 °C degree increase from the background formation temperature (pre-test modeling suggested that full coupling would yield 55 °C). Next, the heater set point was increased stepwise from 120 to 155 to 185 °C, and finally to 220 °C. Although, the temperature rise was less than predicted, these experiments provided valuable data for calibrating and developing numerical models. Next, to increase the thermal coupling between the heater and the formation, a 260-W, 0.6-m-long (22-inch-long) quartz infrared heater was installed on 13 Dec. 2018 (Helios Quartz infrared twin tube, medium wave; Figure 2). On 19 Feb. 2019, the heater was upgraded to a 750-W version. The infrared heaters overcame the insulating layer of air by emitting infrared radiation directly onto the borehole wall. This greatly increased the observed temperatures in the observation boreholes (Figure 3).

3 | MODEL DEVELOPMENT

Model development has been conducted at Los Alamos using the porous medium flow simulator FEHM (Finite Element Heat and Mass transfer code; Zyvoloski et al., 2012; https://fehm.lanl.gov) and at Lawrence Berkeley National Laboratory using the simulator TOUGH-FLAC (Transport Of Unsaturated Groundwater and Heat–Fast Lagrangian Analysis of Continua; Blanco-Martín, Rutqvist, Battistelli, & Birkholzer, 2018; Rutqvist, 2017; https://tough.lbl.gov). The goal of simultaneously developing numerical simulations is to benchmark the models against each other to validate their results. Additionally, TOUGH-FLAC can simulate the large-scale deformation expected around the borehole due to salt creep. Simulations in FEHM using 3D meshes have been conducted for each of the heater tests and will be presented

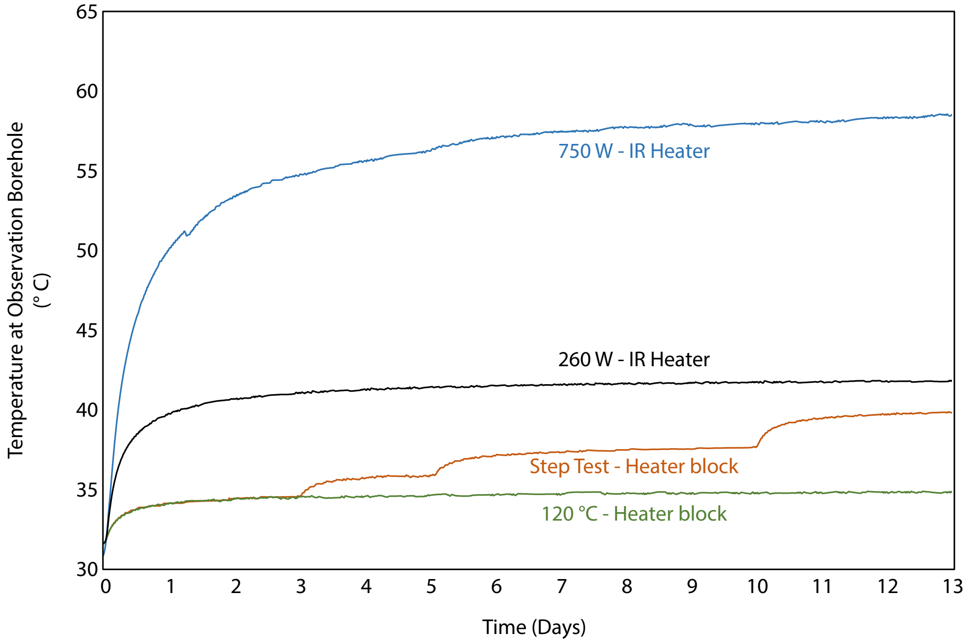

FIGURE 3 Temperature at the borehole sensor at the depth of the heater (TBO) vs. time since heating began during each heater test. The TBO is located ~0.3 m (1 ft) away from the heated borehole. IR, infrared

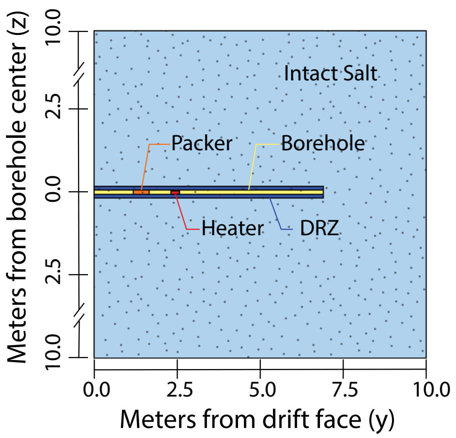

FIGURE 4 Cross-section of the model regions geometry, showing the 0.12-m-radius borehole in yellow, packer in orange, heater in red, the 0.08-m-thick damaged rock zone (DRZ) in dark blue, and the background salt in light blue. The full mesh is 20 × 10 × 20 m and is composed of 1,003,995 elements

first, followed by a comparison to the TOUGH-FLAC simulations using a two-dimensional (2D) axial symmetric mesh that incorporates mechanical deformation.

To simulate the borehole heater experiments using FEHM a 3D mesh was generated using LaGriT (the Los Alamos Grid Toolbox, https://lagrit.lanl.gov). The mesh is 20 × 20 × 10 m (Figures 4 and 5), with the center of borehole lying at $x = 0$, $z = 0$. The mesh is highly refined near the borehole and the resolution decreases radially. This results in a mesh of 1,003,995 elements. The high refinement near the borehole helps resolve steep temperature, saturation, and pressure gradients near the borehole wall.

Beginning with appropriate initial conditions is critical to model accuracy. The results of 30 previous permeability experiments conducted at WIPP show that the typical average anhydrite permeability ranges from 10^{-18} to 10^{-20} m^2, whereas average halite permeability is $<10^{-20}$ (Beauheim & Roberts, 2002). Pressure testing of recently drilled boreholes suggest the DRZ around boreholes has a permeability of ~10^{-18} m^2. Through model fitting, we find that an initial permeability of 10^{-21} m^2 for intact salt and 10^{-18} m^2 for the borehole DRZ accurately reflects the water production during the experiments. A linear capillary pressure and relative permeability model is used for the intact salt and DRZ, with capillary pressure varying between 0 MPa when fully saturated and 1 MPa at a theoretical zero saturation (Johnson et al., 2019). Table 1 lists the initial properties of the intact salt, DRZ, and borehole used during the simulations. These values were sourced from the literature: salt permeability, formation pressure, and salt porosity (Beauheim & Roberts, 2002), relative permeability function (Johnson et al., 2019), as well as our field measurements (DRZ permeability, formation temperature, and N_2 flow rate). These properties evolve during the simulation. For instance, porosity changes due to the dissolution of salt, which causes changes in permeability, whereas temperature changes from the heater drive changes in thermal conductivity. The implementation of these coupled processes in FEHM has been developed over the past 8 yr, with many of these functions described in recent work by Harp, Stauffer, Mishra, Levitt, and Robinson (2014), Jordan,

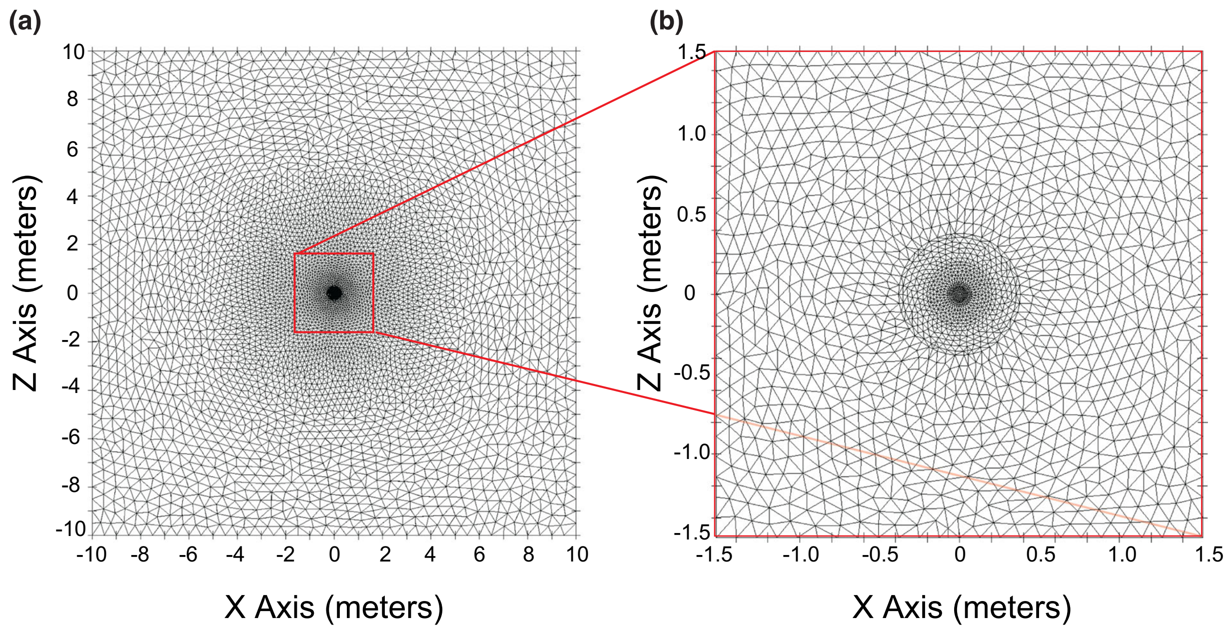

FIGURE 5 Cross-section of model domain parallel to drift face. (a) 20-m × 20-m domain (b) 3-m × 3-m subsection centered around the borehole

TABLE 1 Key initial parameters used for heated borehole simulations

Parameter (units)	Value
Salt initial porosity (–)	0.001
Salt initial permeability (m^2)	10^{-21}
Damaged rock zone permeability (m^2)	10^{-18}
Damaged rock zone thickness (m)	0.08
Borehole permeability (m^2)	10^{-12}
Packer permeability (m^2)	10^{-26}
Salt thermal conductivity at 31.5 °C (W m^{-1} K^{-1})	5.25
Air thermal conductivity (W m^{-1} K^{-1})	0.03
Initial formation pressure (MPa)	12
Initial formation temperature (°C)	31.5
Air source behind heater (kg s^{-1})	3.83×10^{-6}
Residual saturation (–)	0.1
Maximum capillary pressure (MPa)	1.0
Saturation at which capillary pressure is zero (–)	1.0

Boukhalfa, Caporuscio, and Stauffer (2015), Johnson et al. (2018), and Johnson et al. (2019).

Due to the extremely low permeability and porosity of intact salt, field measurements of formation brine pressure and saturation are difficult. Because salt cannot resist deviatoric stress, the far field formation pressure at WIPP should approach the lithostatic stress (15 MPa); however, experiments have shown that the formation pressure in the near field is likely less due to the stress relief provided by the WIPP excavation and may be around 12 MPa (Beauheim et al., 1999; Beauheim & Roberts, 2002). Using this information and knowledge of the mining activities at WIPP, we simulate an estimated pressure and saturation distribution at the location of the heated borehole in the E-140 drift. First, the model is initialized at 12 MPa throughout the domain; this represents the formation prior to the excavation of the mine (Figure 6). Next, an atmospheric pressure boundary condition and nearly dry saturation of 0.01 is applied along one side; these boundary conditions represent the initial mining of the E-140 drift in 1982. A 12-MPa and fully saturated boundary condition is applied on the top, bottom, and back walls, which represent the background far-field conditions at WIPP. Next, the model is allowed to equilibrate for 30 yr. After 30 yr of model time, the domain is further updated to include the borehole; this corresponds to the drilling of the boreholes shown in Figure 2 in 2012. To include the borehole, the porosity of this section of the model is set to 99.999% and the permeability is set to 10^{-12} m^2. A saturation of 0.01 and atmospheric pressure boundary condition is maintained at the drift wall, and the model is run for an additional 6 yr to arrive at the unsteady pressure and saturation condition within the formation at the start of the heater testing. This long-term modeling processes results in reduced pressure and saturations around the borehole, which limit the thermal pressurization. However, in freshly drilled boreholes where the pressure and saturation have not equilibrated, thermal pressurization may still largely contribute to brine availability.

During the experiment, dry N_2 was injected behind the heater at 200 ml min^{-1}, the N_2 picked up moisture and exited through an outlet in the packer. We simulate this as a dry air

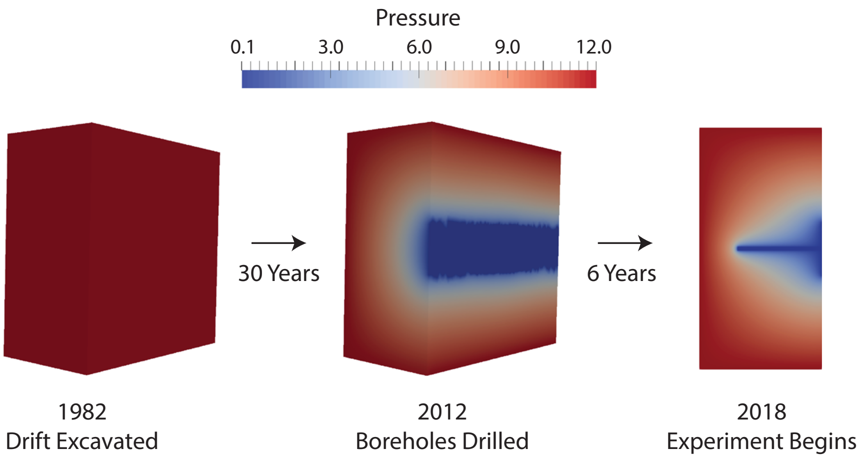

FIGURE 6 Brine pore pressure (in MPa) distribution development for simulation initialization. Domain is 20 × 10 × 20 m

source located ~0.2 m past the heater with an equivalent flow rate of 3.83×10^{-6} kg s^{-1}. The dry air picks up humidity and exits the model at a node located at the packer surface with an atmospheric pressure condition. The packer is given a permeability of 10^{-26} m^2, and a distributed energy flux is used to simulate the infrared heaters, while a constant temperature boundary condition is used to represent the stainless steel heater.

Thermal properties of the salt formation can be determined through experimentation and modeling of time-dependent temperature response to the heater in adjacent boreholes. The thermal conductivity of intact salt is a function of temperature and is described by

$$K_T(T) = K_{T\text{-}300}\left(\frac{300}{T}\right)^{1.14} \quad (1)$$

where T is temperature (K) and $K_{T\text{-}300}$ is the thermal conductivity of pure halite at 300 K (5.4 W m^{-1} K^{-1}) (Johnson et al., 2019; Munson et al., 1990). Initial simulations of the experiment assumed full coupling between the heater and the heated borehole wall. However, these preliminary simulations overpredicted the transfer of heat into the formation. To address the discrepancy between the simulated and measured temperatures, the simulations were modified to add an air gap around the heater in the heated borehole. While the fully coupled simulation assumed tight contact between the borehole wall and the heater, the heater simulations including the air gap assumed only direct contact between the heater and the salt on the bottom of the heated borehole where the heater rests. This air gap was an effective insulator around the heater. Results of the final constant 120 °C heater simulation temperature are shown in Figure 7. The model is able to represent the temperature at the monitoring locations to within 1 °C. In our conceptualization, the heater is resting on the bottom of the borehole making TSBO (TSB temperature sensor at position 0, the same depth as the heater) 24 cm from the heater, whereas TBO (TB temperature sensor at position 0) is 29 cm away. In addition, the contact between the heater and salt increases the temperature beneath the heater, resulting in a warm TSBO. Some error is likely associated with measuring the precise locations of the temperature sensors within boreholes and deviation of boreholes from horizontal. Each borehole is not perfectly straight and level, and some movement of the temperature sensors during installation and grouting is possible. Other sources of error include that the manner in which the heater is making contact with the salt may differ from our conceptualization, and that in these simulations we are neglecting black body radiation from the heater.

3.1 | Variable-temperature heater block simulations

As stated earlier, in an attempt to reach the target formation temperature of 120 °C, the heater block temperature was raised in a stepwise fashion while monitoring the temperature in adjacent boreholes. The heater block controller was set at 120, 155, 185, and 220 °C over the course of 40 d (Figure 8).

Using the same constant thermal conductivity (K_{air} = 0.03 W m^{-1} K^{-1}) for the insulating air around the heater block, we found that the simulations underestimated the borehole temperatures by a few degrees (yellow line, Figure 8). In order to accurately produce the higher temperatures associated with this experiment, a new variable conductivity algorithm was added to the FEHM source code. This update approximates radiative energy transfer from a black body between two nodes through an adjustment of the thermal conductivity. The energy flux due to black body radiation is proportional to the difference in the temperature to the fourth power (Equation 2) (Jordan, 2015; Kreith & Bohn, 1993)

$$q_{rad} = A_1 F_{1-2} \sigma \left(T_1^4 - T_2^4\right) \quad (2)$$

where A_1 is the surface area of the heater (m^2), T_1 is the temperature of the heater (K), T_2 is the temperature of the borehole wall, F_{1-2} is a shape factor, and σ is the emissivity of

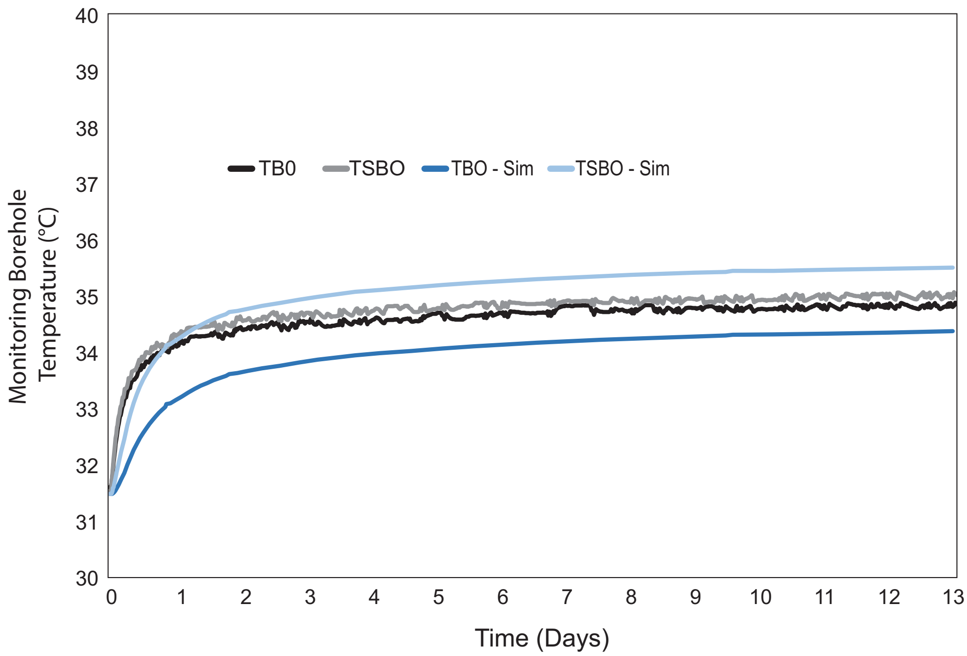

FIGURE 7 Final simulation of the 120 °C heater block experiment. Observations are black and gray, and model predictions are blue. TBO, temperature borehole sensor at the depth of the heater; TSBO, temperature small borehole sensor at the depth of the heater; TBO-Sim, simulated temperature at TBO; TSBO-Sim, simulated temperature at TSBO

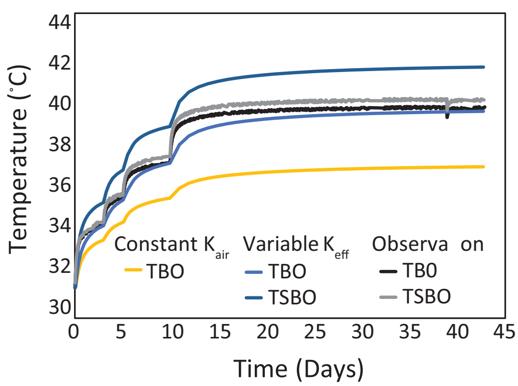

FIGURE 8 Variable temperature heater block simulation. Yellow line indicates simulation of the temperature at the temperature borehole (TB) without accounting for radiative transfer from the heater block. Observations are black and gray lines. K_{air}, constant thermal conductivity; K_{eff}, effective thermal conductivity; TBO, temperature borehole sensor at the depth of the heater; TSBO, temperature small borehole sensor at the depth of the heater.

the stainless steel heater (W m^{-2} K^{-4}). In this case, the shape factor is 1, since all of the radiation from the heater impacts the salt. Using this energy flux, we can determine the change in thermal conductivity necessary to account for the radiation, K_R, as

$$K_R = \frac{q_{rad} H}{A_1 \left(T_1 - T_2\right)} \tag{3}$$

where H is the distance of the air gap in the borehole. Finally, the effective thermal conductivity is the sum of the thermal properties of the air and those due to radiation:

$$K_{eff} = K_R + K_{air} \tag{4}$$

Applying this variable thermal conductivity model, we achieved a satisfactory match to the experimental data (Figure 8). Some error is likely due to the location of the temperature sensors and position of the heater, as mentioned above, as well as the selection of an appropriate emissivity factor, which varies by material, temperature, and over time. Unfortunately, even with the steel block heater set to 220 °C, the observation boreholes only achieved about 40 °C.

3.2 | Radiative heating experiments and simulations

The radiative heating experiments are modeled using a fully coupled heater (no air gap), and a Neumann-style (constant) energy flux boundary condition (Figure 9).

The 260-W heater was placed at approximately the same depth into the borehole as the block heater; however, the 750-W heater was placed deeper into the heated borehole, causing the TSB temperature sensor to be out of plane with the heater. This reduces the temperature observed at TSB, even though the overall energy flux into the formation was significantly higher. At the TB observation point, the

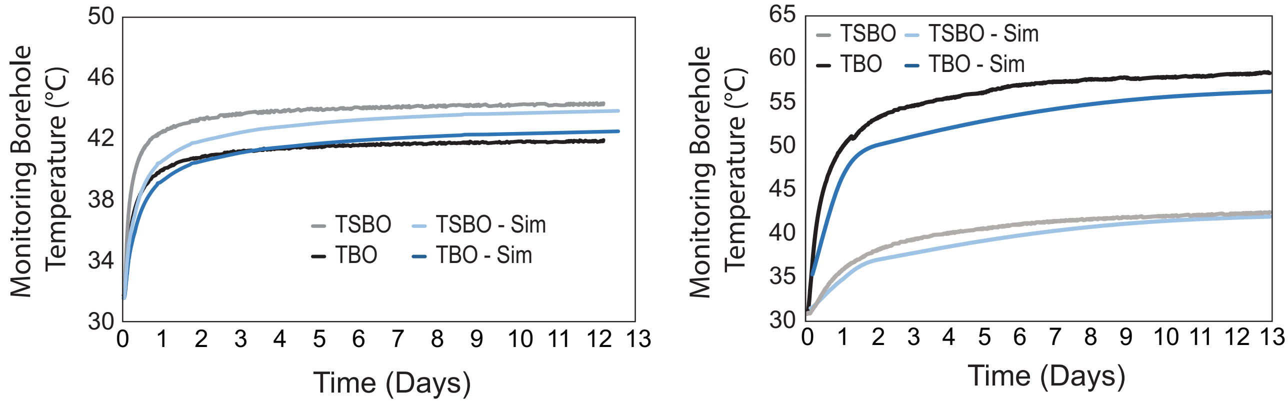

FIGURE 9 (A) Simulation of 260-W infrared heater and (B) 750-W infrared heater experiment. TBO, temperature borehole sensor at the depth of the heater; TSBO, temperature small borehole sensor at position the depth of the heater; TBO-Sim, simulated temperature at TBO; TSBO-Sim, simulated temperature at TSBO

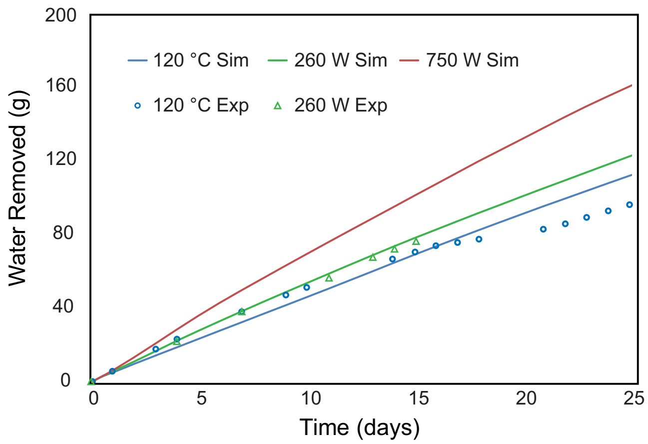

FIGURE 10 Water production during the 120 °C heater block and 260-W radiative heating experiment (exp) compared with simulations (sim). Observations from desiccant are points while simulations are lines

temperature was raised ∼28 °C, and in the salt adjacent to the heater, temperatures reached 144 °C. Reaching the target temperature of 120 °C with the 750-W infrared heater and closely matching the measured data with simulations provides confidence in our ability to simulate important experimental design parameters during the larger scale experiments.

3.3 | Brine availability

The experimental measurements of water production compared to the FEHM simulations are presented in Figure 11. Due to drying of the DRZ around the borehole from the mine ventilation over the 6 yr between borehole drilling and testing, the water production from these tests is expected to be less than the water production from fresh boreholes. The simulation predicts the DRZ above the heater is ∼38% saturated and the DRZ below the heater is ∼50% saturated, with the difference being due to gravity (Figure 11). During heating, the increased vapor pressure near the heater drives the remaining water out of the DRZ and, to some extent, out of the nearby intact salt. This results in increased water production with increased heat. Simulations suggest that total draining of the nearby DRZ happens quickly; however, draining the entire DRZ does not happen within 3 yr of model simulation and will likely take many years.

After ∼550 d of simulation, water ponds in the borehole behind the air inflow point, extending to the rear of the borehole (Figure 11). Once this ponded water approaches the air source, the air humidity is increased and more water is removed from behind the packer. This changes the trend line from one where the only source of water is water that reaches the borehole between the packer and the air source to one where water is being sourced from the entire borehole behind the packer (Figure 12). This “early water” is produced at ∼4.8 g d^{-1}, whereas the “late water” is produced at 8.5 g d^{-1}. This finding emphasizes the impact that the size of the borehole and the location of the air injection have on water production. Placement of the air source at the end of the borehole would likely eliminate this result and, in general, longer boreholes will produce more water than shorter boreholes.

During active waste emplacement of heat-generating waste, the DRZ around newly mined waste disposal drifts and boreholes may be more saturated than the older boreholes used as part of this field test. The planned Phase 1 BATS experiment will be conducted in new boreholes to examine the response of a more fully saturated DRZ to heat. Assuming the same conditions as in the above simulations but with a completely saturated DRZ, the models predict an additional inflow of 150 g of water (9%) during the first year as additional water drains from the DRZ (Figure 13). It is likely that during actual waste emplacement activities, the initial increase in brine flow to the

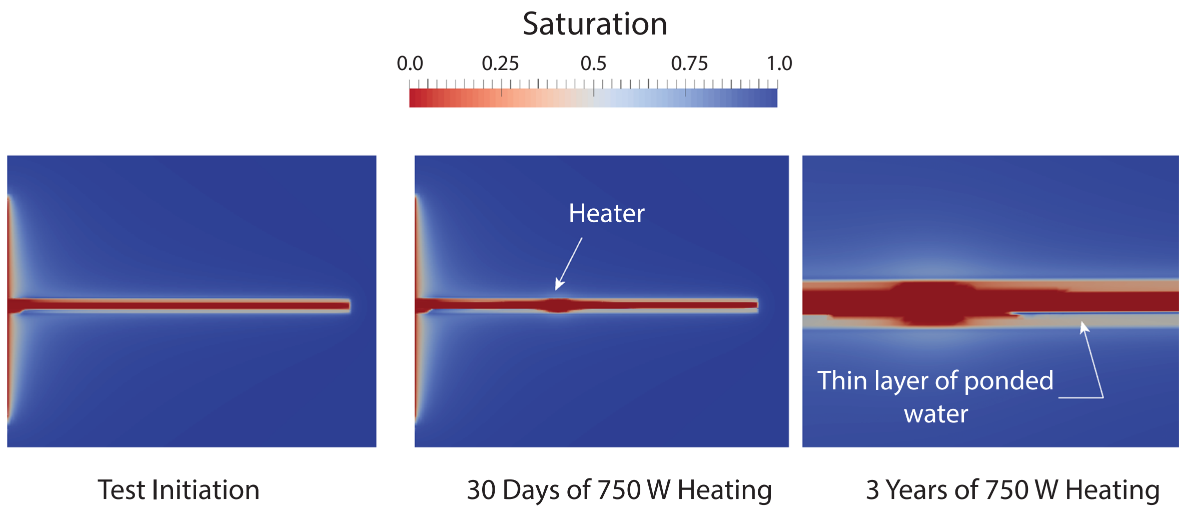

FIGURE 11 Initial saturation condition at the start of testing (left), 30 d after 750-W radiative heating (center), and after 3 yr of 750-W heating (right). The heater increases the nearby vapor pressure and drives the remaining saturation out of the nearby damaged rock zone and intact salt. After ~1 yr, water begins to pool behind the air inflow point

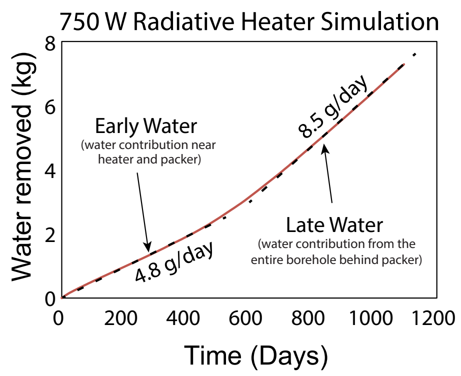

FIGURE 12 Long-term water production during a 750-W radiative heating simulation of the shakedown test. Two linear trends are identified: an early trend at 4.8 g d^{-1}, which is controlled by water sourced between the packer and the air source, and a late trend at 8.5 g d^{-1}, which receives water from the entire borehole through ponded water, which accummulates and reaches the air source at ~550 d

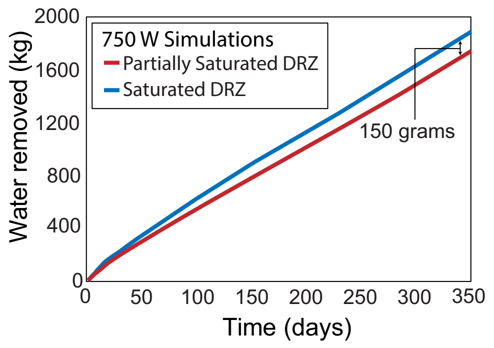

FIGURE 13 A comparison of water production from a borehole with a saturated damaged rock zone (DRZ, freshly drilled) and one with the saturation profile developed by long-term simulation

waste canisters could be avoided by constructing drifts and/or boreholes with a modest lead time.

The two responses in Figure 13 likely overestimate and underestimate the brine production from a fresh borehole. The mechanism that creates the increased porosity and permeability in the DRZ also lowers the saturation, since new brine cannot flow in quickly to fill up this newly created porosity. This can result in a delay in water intrusion as this saturation is filled. At the drift scale, simulations predict this process to increase porosity by ~10% of its initial value near the drift wall and 1% up to 0.55 m from the drift wall (Freeze et al., 1997). This process and evaporation within the drift combined to prevent the observation of flow into a newly excavated room for 2 yr (Freeze et al., 1997). These results are dependent on the size of the DRZ. Around the drift, the DRZ extends about 0.5–1.5 m into the rock (Tsang, Bernier, & Davies, 2005), but this is a function of the size of the drift excavation that is ~5 m in height and width. In our simulations, the DRZ extends ~0.08 m (~3 inches) around the 0.12-m-radius (4.8-inch-radius) borehole. The lack of evaporation and smaller DRZ mean the water production into a freshly drilled borehole will begin more quickly than in rooms and drifts.

3.4 | Model comparison of TOUGH-FLAC and FEHM simulations

Thermo–hydro–mechanical simulations of the experiment using the TOUGH-FLAC simulator (Blanco-Martín et al., 2018; Rutqvist, 2017) have been carried out by the Lawrence Berkeley National Laboratory (Rutqvist et al., 2019). The TOUGH-FLAC simulations, which incorporate the

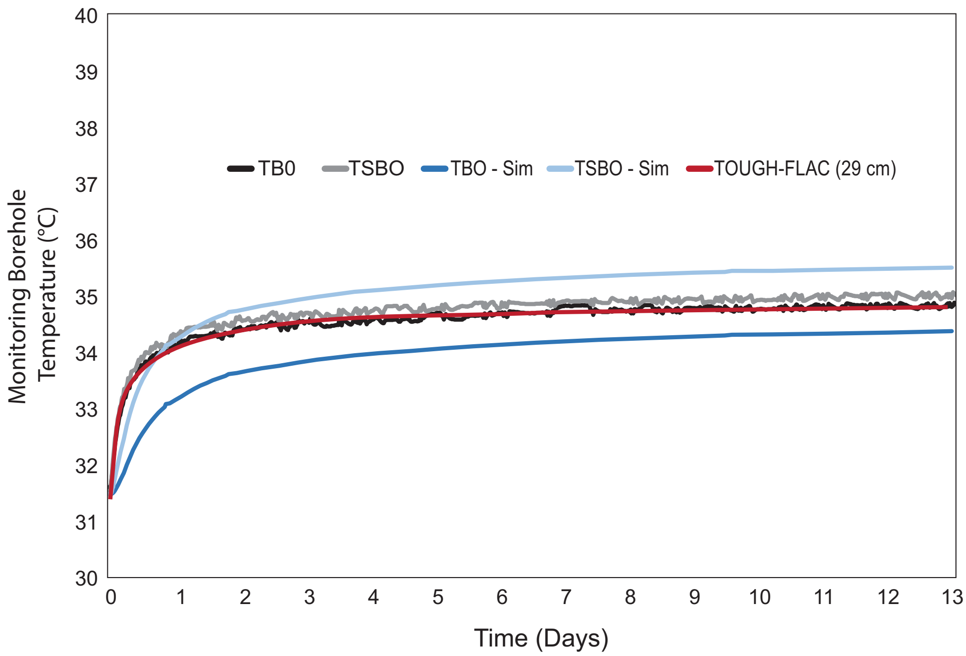

FIGURE 14 Comparison between the temperature predicted at the temp small borehole sensor at the depth of the heater (TSBO) and temperature borehole sensor at the depth of the heater (TBO) during the constant 120 °C heater block using FEHM (Finite Element Heat and Mass transfer code) to the two-dimensional axial symmetric TOUGH-FLAC (Transport Of Unsaturated Groundwater and Heat–Fast Lagrangian Analysis of Continua) model at 29 cm. TBO-Sim, simulated temperature at TBO; TSBO-Sim, simulated temperature at TSBO.

viscoplastic mechanical deformation of salt, are computationally expensive and have been conducted representing the borehole experiment using a 2D axial symmetric mesh geometry, which is a geometric simplification compared with the 3D FEHM mesh. The thermal and hydraulic properties are equal to those used in FEHM and presented in Table 1. As in the FEHM modeling, an initial fluid pressure and temperature was set to 12 MPa and 31.5 °C. An atmospheric pressure is applied at the borehole wall, and the inflowing water mass and temperature evolution are simulated and compared with experimental data and FEHM modeling results. The temperature profiles between FEHM and TOUGH-FLAC are within 1 °C of the experimental data (Figure 14). As conceptualized in the FEHM resistive heater models, the heater is resting on the bottom of the borehole. In this configuration, TSBO is 24 cm from the heater and TBO is 29 cm from the heater. This results in a warmer TSBO than TBO. In the 2D TOUGH-FLAC simulations, temperature was monitored at 29 cm, which is an approximation of the location of the TBO and TSBO temperature monitoring boreholes. An important distinction between these two simulations is the way in which the thermal conductivity in the borehole is handled. The FEHM simulations presented here use a constant $K_{air} = 0.03$ W m^{-1} K^{-1}, whereas the TOUGH-FLAC simulations use a calibrated K_{air} to match the experimental results. This results in a K_{air} value of 0.06 W m^{-1} K^{-1}. The calibration can be justified by considering that the precise location of the heater and sensors is unknown, and the thermal emissivity of the stainless steel heater varies over time and can be difficult to know precisely. Also, in the TOUGH-FLAC 2D axial symmetric model, the heater is assumed to be at the center of the heater borehole and not touching the bottom of the borehole, as it does in the 3D FEMH simulation. Despite these differences, the models perform similarly, which increases our confidence in our ability to predict the temperature evolution in the salt appropriately and thereby provides confidence in the design of future experiments.

The brine flow rates estimated for the 120 °C steel block heater during the FEHM and TOUGH-FLAC simulations also agree, but the FEHM simulations stabilize more quickly at a flow rate of ~4.8 g d^{-1}, whereas the TOUGH-FLAC simulations stabilize closer to 4.3 g d^{-1} (Figure 15). Total water mass removal reflects the differences in flow rate, but overall, both simulations produce a similar result.

The incorporation of viscoplastic constitutive laws in the mechanical simulator FLAC3D (Fast Lagrangian Analysis of Continua in Three Dimensions) allows TOUGH-FLAC to simulate the creep closure of salt from differential stress around the excavation and borehole, as well as the thermal pressurization due to heating. The initial stress at the WIPP site is taken as 14.8 MPa, based on the weight of the overburden rock. The stress field is assumed to be isotropic, which is reasonable as a result of long-term creep deformations (Hansen, 2003).

For creep, the Lux–Wolters constitutive model was used in TOUGH-FLAC, with model parameters previously applied

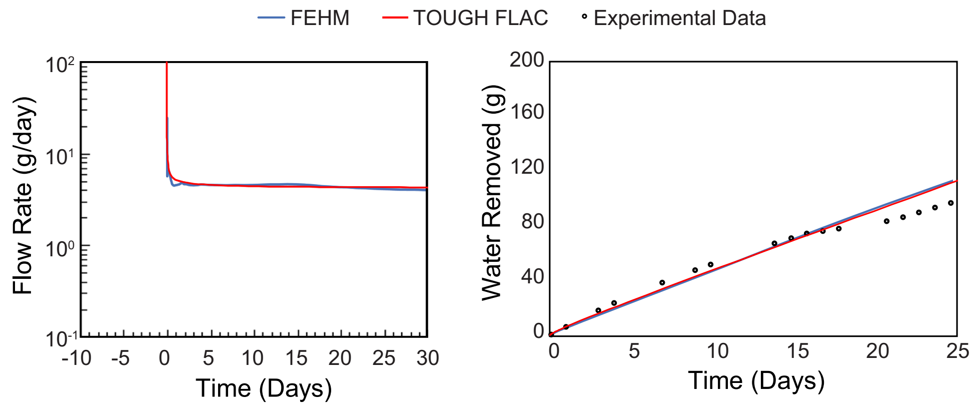

FIGURE 15 Comparison of flow rate (left) and cumulative water removed (right) during the 120 °C steel block heater predicted by the FEHM (Finite Element Heat and Mass transfer code) three-dimensional model and the TOUGH-FLAC (Transport Of Unsaturated Groundwater and Heat–Fast Lagrangian Analysis of Continua) two-dimensional axial symmetric model

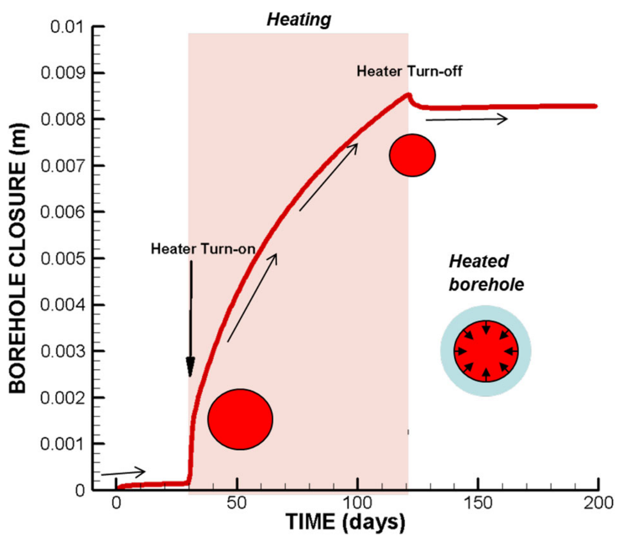

FIGURE 16 Borehole closure due to 750-W heating simulated using TOUGH-FLAC (Transport Of Unsaturated Groundwater and Heat–Fast Lagrangian Analysis of Continua). Data are from Rutqvist et al. (2019)

in TOUGH-FLAC modeling of in situ experiments at Asse Mine in Germany (Blanco-Martín, Wolters, Rutqvist, Lux, & Birkholzer, 2016) and validated for borehole closure from historic field experiments at WIPP (Rutqvist, Blanco-Martin, Hu, & Birkholzer, 2017).

These creep deformation simulations predict only a small amount of closure during the 120 °C heater block experiment. This is because of the short test duration and small amount of heat transmitted into the salt. However, when exposed to a 750-W radiative heater for 90 d, the borehole closure is simulated to be almost 1 cm (Figure 16). During the next round of BATS testing, the closure of the borehole will be monitored by a borehole closure gauge placed near the heater, and the simulations can be compared with experimental results (Mills et al., 2019). Such comparison between modeling and experiments will help to constrain creep parameters for the constitutive viscoplastic model, including parameters for temperature dependency on creep.

4 | CONCLUSION

A USDOE Office of Nuclear Energy-funded collaboration between Sandia, Los Alamos, and Lawrence Berkeley National Laboratories is performing a series of heated borehole experiments underground at WIPP as part of an effort to investigate possibly storing heat-generating nuclear waste in salt formations. The first round of testing showed that a heater mounted in a steel block is poorly suited to delivering energy into the salt formation due to poor thermal coupling; however, these experiments can be accurately modeled once an insulating air gap and radiative heat transfer are incorporated into FEHM. Radiative heaters deliver significantly more energy through the air-filled borehole than a conduction-driven heater block and are capable of reproducing temperatures over 120 °C. Including a DRZ around the borehole within numerical simulations is important for forecasting water production and thermal pressurization due to its potentially lower saturation, higher porosity, and higher permeability. The extremely low permeability of salt means that the initial pressure and saturation condition of these experiments are not uniformly distributed and are not at a steady state. Long-term modeling can be used to develop the appropriate initial pressure and saturation distributions accounting for the atmospheric pressure along the drift wall and boreholes. Agreement on temperature response to within 1 °C and similar water production results from FEHM and TOUGH-FLAC give the team confidence in their ability to simulate upcoming heated borehole experiments. The simulation of water production using an initial permeability of 10^{-21} m^2

suggests the lack of a higher porosity and permeability clay layer within the tested boreholes; however, with limited high-temperature experiments and a lack of isotopic and chemical testing of the brine, it is difficult to discern the potential effect of mobilizing fluid inclusions. These aspects of brine availability will be investigated in future phases of the BATS testing. Data from the next BATS experiment will be used to refine these models further and explore the brine availability to spent fuel waste canisters in freshly drilled boreholes.

ACKNOWLEDGMENTS

We would like to acknowledge the helpful comments received by Dr. Bret Leslie and two anonymous reviewers. This work was supported by the USDOE Office of Nuclear Energy and the Office of Environmental Management through the Los Alamos National Laboratory. The Los Alamos National Laboratory is operated by Triad National Security for the National Nuclear Security Administration of the USDOE (Contract no. 89233218CNA000001). The unclassified release number for the work is LAUR-19-31638. Sandia National Laboratories is a multi-mission laboratory managed and operated by National Technology and Engineering Solutions of Sandia, a wholly owned subsidiary of Honeywell International, for the USDOE's National Nuclear Security Administration under Contract DE-NA-0003525. Funding for Lawrence Berkeley National Laboratory contribution was provided by the Spent Fuel and Waste Science and Technology, Office of Nuclear Energy, of the USDOE under Contract no. DE-AC02-05CH11231 with Lawrence Berkeley National Laboratory.

CONFLICT OF INTEREST

The authors declare no conflict of interest.

ORCID

Eric J. Guiltinan https://orcid.org/0000-0002-0763-0625
Kristopher L. Kuhlman https://orcid.org/0000-0003-3397-3653
Jonny Rutqvist https://orcid.org/0000-0002-7949-9785
Mengsu Hu https://orcid.org/0000-0002-8853-2022
Hakim Boukhalfa https://orcid.org/0000-0001-6383-8503
Melissa Mills https://orcid.org/0000-0002-1011-6977
Shawn Otto https://orcid.org/0000-0002-9018-686X
Douglas J. Weaver https://orcid.org/0000-0003-0358-1923
Brian Dozier https://orcid.org/0000-0001-8356-7042
Philip H. Stauffer https://orcid.org/0000-0002-6976-221X

REFERENCES

Anthony, T. R., & Cline, H. E. (1971). Thermal migration of liquid droplets through solids. *Journal of Applied Physics*, *42*, 3380–3387.

Beauheim, R. L., Ait-Chalal, A., Vouille, G., Tijani, S.-M., McTigue, D. F., Brun-Yaba, C., … Mollema, P. N. (1997). *INTRAVAL phase 2 WIPP 1 test case report: Modeling of brine flow through halite at the waste isolation pilot plant site* (Report SAND97-0788). Albuquerque, NM: Sandia National Laboratories.

Beauheim, R. L., Domski, P. S., & Roberts, R. M. (1999). *Hydraulic testing of Salado Formation evaporites at the waste isolation pilot plant site: Final report* (Report SAND98-2537). Albuquerque, NM: Sandia National Laboratories.

Beauheim, R. L., & Roberts, R. M. (2002). Hydrology and hydraulic properties of a bedded evaporite formation. *Journal of Hydrology*, *259*, 66–88. https://doi.org/10.1016/S0022-1694(01)00586-8

Blankenship, D. A., & Stickney, R. G. (1983). *Nitrogen gas permeability tests at Avery Island* (Report ONWI- 190(3)). Columbus, OH: Office of Nuclear Waste Isolation.

Blanco-Martín, L., Rutqvist, J., Battistelli, A., & Birkholzer, J. T. (2018). Coupled processes modeling in rock salt and crushed salt including halite solubility constraints: Application to disposal of heat-generating nuclear waste. *Transport in Porous Media*, *124*, 159–182. https://doi.org/10.1007/s11242-018-1057-7

Blanco-Martín, L., Wolters, R., Rutqvist, J., Lux, K.-H., & Birkholzer, J. T. (2016). Thermal–hydraulic–mechanical modeling of a large-scale heater test to investigate rock salt and crushed salt behavior under repository conditions for heat-generating nuclear waste. *Computers and Geotechnics*, *77*, 120–133. https://doi.org/10.1016/j.compgeo.2016.04.008

Bourret, S. M., Guiltinan, E. J., Johnson, P. J., Otto, S., Weaver, D. J., Dozier, B., … Stauffer, P. H. (2019). Experiments and simulation of a borehole in salt to understand heat, brine, and vapor migration. In *Waste Management 2019 Proceedings*. Red Hook, NY: Curran Associates.

Bradshaw, R. L., & McClain, W. C. (1971). *Project Salt Vault: A demonstration of the disposal of high- activity solidified wastes in underground salt mines*. (ORNL-4555). Oak Ridge, TN: Oak Ridge National Laboratory.

Bredehoeft, J. D. (1988). Will salt repositories be dry? *EoS*, *69*, 121–131. https://doi.org/10.1029/88EO00078

Coyle, A. J., Eckert, J., & Kalia, H. (1987). *Brine Migration test report: Asse Salt Mine, Federal Republic of Germany* (Report BMI/ONWI-624). Columbus, OH: Office of Nuclear Waste Isolation, Battelle Memorial Institute.

Deal, D. E., Abitz, R. J., Belski, D. S., Case, J. B., Crawley, M. E., Givens, C. A., … Valdivia, M. A. (1995). *Brine sampling and evaluation program 1992–1993 report and summary of BSEP data since 1982* (Report DOE-WIPP 94-011). Carlsbad, NM: Westinghouse Electric Corporation.

Finley, S. J., Hanson, D. J., & Parsons, R. (1992). *Small-scale brine inflow experiments: Data report through 6/6/91* (Report SAND91-1856). Albuquerque, NM: Sandia National Laboratories.

Freeze, G. A., Christian-Frear, T. L., & Webb, S. W. (1997). *Modeling brine inflow to Room Q: A numerical investigation of flow mechanisms* (Report SAND96-0561). Albuquerque, NM: Sandia National Laboratories.

Geckeis, H., & Klenze, R. (2009). *Institute for nuclear waste disposal annual report 2008*. Karlsruhe, Germany: Institut für Nukleare Entsorgung.

Hansen, F. D. (2003). *The disturbed rock zone at the waste isolation pilot plant* (Report SAND2003-3407). Albuquerque, NM: Sandia National Laboratories.

Hansen, F. D., & Leigh, C. D. (2011). *Salt disposal of heat-generating nuclear waste* (Report SAND2011-0161). Albuquerque, NM: Sandia National Laboratories.

Harp, D. R., Stauffer, P. H., Mishra, P. K., Levitt, D. G., & Robinson, B. A. (2014). Thermal modeling of high-level nuclear waste disposal in a salt repository. *Nuclear Technology*, *187*, 294–307, https://doi.org/10.13182/NT13-110

IAEA. (2018). *Status and trends in spent fuel and radioactive waste management*. Vienna: International Atomic Energy Agency.

Johnson, P. J., Otto, S., Weaver, D. J., Dozier, B., Miller, T. A., Jordan, A. B., … Stauffer, P. H. (2019). Heat-generating nuclear waste in salt: Field testing and simulation. *Vadose Zone Journal*, *18*(1). https://doi.org/10.2136/vzj2018.08.0160

Johnson, P. J., Stauffer, P. H., Zyvoloski, G. A., & Bourret, S. M. (2018). *Experiments and modeling to support field test design* (Report LA-UR-18-28189). Los Alamos, NM: Los Alamos National Laboratory.

Jordan, A. B. (2015). *Multiphase, multicomponent flow and transport models for Nuclear Test-Ban Treaty monitoring and nuclear waste disposal applications* (Doctoral dissertation). Socorro: New Mexico Institute of Mining and Technology.

Jordan, A. B., Boukhalfa, H., Caporuscio, F. A., & Stauffer, P. H. (2015). *Brine transport experiments in granular salt* (Report LA-UR-15-26804). Los Alamos, NM: Los Alamos National Laboratory.

Krause, W. B. (1983). *Avery island brine migration tests: Installation, operation, data collection, and analysis* (Report ONWI-190(4)). Rapid City, SD: Re/Spec.

Kreith, F., & Bohn, M. S. (1993). *Principles of heat transfer* (5th ed). St. Paul, MN: West Publishing Company.

Krumhansl, J. L., Stein, C. L., Jarrell, G. D., & Kimball, K. M. (1991). *Summary of WIPP room B heater test brine and backfill material data* (Report SAND90-0626). Albuquerque, NM: Sandia National Laboratories.

Kuhlman, K. L. (2019). *Processes in salt repositories* (Report SAND2019-6441R). Albuquerque, NM: Sandia National Laboratories.

Kuhlman, K. L., & Malama, B. (2013). *Brine flow in heated geologic salt* (Report SAND2013-1944). Albuquerque, NM: Sandia National Laboratories.

Kuhlman, K. L., Mills, M. M., & Matteo, E. N. (2017). *Consensus on intermediate scale salt field test design* (Report SAND2017-3179R). Albuquerque, NM: Sandia National Laboratories.

Kuhlman, K. L., & Sevougian, S. D. (2013). *Establishing the technical basis for disposal of heat-generating waste in salt* (FCRD-UFD-2013-000233, SAND2013–6212P). Albuquerque, NM: Sandia National Laboratories.

Larson, K. W. (2000). Development of the conceptual models for chemical conditions and hydrology used in the 1996 performance assessment for the Waste Isolation Pilot Plant, *Reliability Engineering & System Safety*, *69*, 59–86. https://doi.org/10.1016/S0951-8320(00)00025-9

MacKinnon, R. J., Sevougian, S. D., Leigh, C. D., & Hansen, F. D. (2012). *Towards a defensible safety case for deep geologic disposal of DOE HLW and DOE SNF in bedded salt* (Report SAND2011-6032). Albuquerque, NM: Sandia National Laboratories.

McTigue, D. F. (1986). Thermoelastic response of fluid-saturated porous rock. *Journal of Geophysical Research*, *91*, 9533–9542, https://doi.org/10.1029/JB091iB09p09533

McTigue, D. F., & Nowak, E. J. (1987). *Brine transport studies in the bedded salt of the Waste Isolation Pilot Plant (WIPP)* (Report SAND87-1274C). Albuquerque, NM: Sandia National Laboratories.

Mills, M., Kuhlman, K., Matteo, E., Herrick, C., Nemer, M., Heath, J., … Crandall, D. (2019). *Salt heater test (FY19), Rev 2* (Report SAND2019-10240R). Albuquerque, NM: Sandia National Laboratories.

Munson, D. E., Jones, R. L., Ball, J. R., Clancy, R. M., Hoag, D. L., & Petney, S. V. (1990). *Overtest for simulated defense high-level waste (Room B): In situ data report (May 1984–February 1988), Waste Isolation Pilot Plant (WIPP) thermal/structural interactions program* (Report SAND-89-2671). Albuquerque, NM: Sandia National Laboratories.

Nowak, E. J., & McTigue, D. F. (1988). *Interim results of brine transport studies in the Waste Isolation Pilot Plant (WIPP)* (Report SAND87-0880). Albuquerque, NM: Sandia National Laboratories.

Pigford, T. H. (1982). Migration of brine inclusions in salt. *Nuclear Technology*, *56*, 93–101, https://doi.org/10.13182/NT82-A32883

Rothfuchs, T., Wieczorek, K., Feddersen, H. K., Staupendahl, G., Coyle, A. J., Kalia, H., & Eckert, J. (1988). *Brine migration test: Asse Salt Mine Federal Republic of Germany final report* (Report GSF-Bericht 6/88). Joint project between Office of Nuclear Waste Isolation (ONWI) and Gesellschaft für Strahlen und Umweltforschung Munchen (GSF).

Rutqvist, J. (2017). An overview of TOUGH-based geomechanics models. *Computational Geosciences*, *108*, 56–63. https://doi.org/10.1016/j.cageo.2016.09.007

Rutqvist, J., Blanco-Martin, L., Hu, M., & Birkholzer, J. (2017). *Coupled THM modeling in support of a phased salt field test plan*. (SFWD-SFWST-2017-000103, LBNL-2001023). Berkeley, CA: Lawrence Berkeley National Laboratory.

Rutqvist, J., Wu, Y., Hu, M., Commer, M., Wang, J., & Birkholzer, J. (2019). *Salt coupled THMC processes research activities at LBNL: FY2019 progress* (Report LBNL-2001230). Berkeley, CA: Lawrence Berkeley National Laboratory.

Sandia National Laboratories (SNL), Los Alamos National Laboratory (LANL), & Lawrence Berkeley National Laboratory (LBNL). (2020). *Project plan: salt in situ heater test*. (Report SAND2020-1251R). Albuquerque, NM: Sandia National Laboratories.

Stauffer, P. H., Jordan, A. B., Weaver, D. J., Caporuscio, F. A., Ten Cate, J. A., Boukhalfa, H., … Birkholzer, J. T. (2015). *Test proposal document for phased field thermal testing in salt* (Report FCRD-UFD-2015-000077). Los Alamos, NM: Los Alamos National Laboratory.

Sweet, J. N., & McCreight, J. E. (1983). Thermal conductivity of rocksalt and other geologic materials from the site of the proposed waste isolation pilot plant. In D.C. Larsen (Ed.), *Thermal conductivity 16* (pp. 61–78). Boston, MA: Springer. https://doi.org/10.1007/978-1-4684-4265-6_7

Tsang, C. F., Bernier, F., & Davies, C. (2005). Geohydromechanical processes in the excavation damaged zone in crystalline rock, rock salt, and indurated and plastic clays: In the context of radioactive waste disposal. *International Journal of Rock Mechanics and Mining Sciences*, *42*, 109–125. https://doi.org/10.1016/j.ijrmms.2004.08.003

Used Fuel Disposition Campaign (UFD Campaign). (2012). *Used Fuel Disposition Campaign disposal research and development roadmap*

(FCR&D-USED-2011-000065 Rev 1). Lemont, IL: Argonne National Laboratory.

Zyvoloski, G. A., Robinson, B. A., Dash, Z. V., Kelkar, S., Viswanathan, H. S., Pawar, R. J., … Chu, S. P. (2012). *Software users manual (UM) for the FEHM Application Version 3.1-3.X* (Report LA-UR-12-24493). Los Alamos, NM: Los Alamos National Laboratory.

How to cite this article: Guiltinan EJ, Kuhlman KL, Rutqvist J, et al. Temperature response and brine availability to heated boreholes in bedded salt. *Vadose Zone J*. 2020;19:e20019. https://doi.org/10.1002/vzj2.20019